Experimental realization of metastable target skyrmion states in continuous films

Elizabeth M. Jefremovas,[1, a)] Noah Kent,[2] Jorge Marqués–Marchán,[3] Miriam G. Fischer,[1] Agustina Asenjo,[3] and Mathias Kläui[1]

[1)]*Institute of Physics, Johannes Gutenberg University Mainz, Staudingerweg 7, 55128 Mainz, Germany*

[2)]*Research Laboratory of Electronics, Massachusetts Institute of Technology, Cambridge, MA, United States of America*

[3)]*Institute of Materials Sciences of Madrid – CSIC, 28049 Madrid, Spain*

Target skyrmions (TSks) are topological spin textures where the out-of-plane component of the magnetization twists an integer number of k-π rotations. Based on a magnetic multilayer stack in the form of $n\times$[CoFeB/MgO/Ta], engineered to host topological spin textures via dipole and DMI energies, we have stabilized 1π, 2π and 3π target skyrmions by tuning material properties and thermal excitations close to room temperature. The nucleated textures, imaged via Kerr and Magnetic Force Microscopies, are stable at zero magnetic field and robust within a range of temperatures (tens of Kelvin) close to room temperature (RT = 292 K) and over long time scales (months). Under applied field (mT), the TSks collapse into the central skyrmion core, which resists against higher magnetic fields ($\approx 2\times$ TSk annihilation field), as the core is topologically protected. Micromagnetic simulations support our experimental findings, showing no TSk nucleation at 0 K, but a $\approx$ 30 % probability at 300 K for the experimental sample parameters. Our work provides a simple method to tailor spin textures in continuous films, enabling free movement in 2D space, creating a platform transferable to technological applications where the dynamics of the topological textures can be exploited beyond geometrical confinements.

Magnetic skyrmions are topological solitons with potential applications in spintronic devices, owing to their size, mobility and topological stabilization[1–4]. Along with skyrmions, further chiral magnetic topological spin textures have gathered the interest from the scientific community, such as merons or target skyrmions (TSks)[5–7]. The latter k–π vortices, experimentally demonstrated in the last decade, differ from skyrmions by the higher magnetization twists along the z component, quantified by $k > 1$ [see Fig. 1**a**]. Beyond their fundamental interest, an even number of rotations k leads to a trivial topological charge, as defined by the winding number $\mathscr{W} = \frac{1}{4\pi}\int dxdy\ \vec{m}\ (\partial_x\vec{m}\ \partial_y\vec{m})$. In the absence of topological charge, there is no skyrmion Hall effect, which is advantageous for current–driven technology applications[8–13]. Furthermore, the polarity of a TSk can be easily switched by means of AC field, which provides an additional control parameter in spintronics applications[14].

In the recent years, TSks have also enabled the experimental realization of 3D spin textures, as they serve as *hopfion precursors*[15]. These topological 3D solitons, together with other recently discovered structures like skyrmion cocoons[16], are the result of the expansion into the 3rd dimension of 2D topological textures, a groundbreaking research field hosting exciting unique physical phenomena and potential applications in magnetic sensor and information processing technologies[15–19]. There is, however, an open challenge in the experimental stabilization of 3D solitons for technological applications. Up to date, the preferred strategy relies on the lateral confinement of the structures (typically, in a nanodisk shape). This procedure, although prosperous for stabilizing hopfions[15], actually prevents the free motion of the soliton in the whole continuous film, hampering their foreseen computing applications, as the information carriers need to freely move in space[20,21].

Here, we report a magnetic multilayer stack, capable of hosting target skyrmions with and without finite topological charge (1π and 3π, and 2π-type) in the continuous film. The TSks are activated through temperature fluctuations close to room temperature (RT = 292 K), being stable in a range of temperatures close to RT and zero field. In addition to this, we report an increase of the energy barrier of such metastable states with the magneto-dipolar coupling strength, scaled up by increasing the number of repetitions of the multilayer (n = 2, 3, 4, 7, 12). To ensure the technological transfer of our results, the multilayer stack is designed so as the metastable TSk states can be reached at temperature values in agreement with the working range of technological devices (*i.e.*, from 314 K up to 380 K), which validates our method for application perspectives.

We have designed a magnetic multilayer stack in the form of Ta(4)/[$Co_{20}FeCo_{60}B_{20}$(0.86)/MgO(2)/Ta(2)]$_n$, being n = 2, 3, 4, 7 and 12. Numbers in brackets indicate the layer thickness, in nm. The Ta/CoFeB interface provides the interfacial Dzyaloshinskii-Moriya interaction (DMI), while the CoFeB/MgO interface is the source of the perpendicular magnetic anisotropy (PMA) of the stack. A schematic representation of the stack can be visualized in Fig. 1**b**. Details on the specific stack parameters are included in the Supplementary Material. To image the TSks, we have employed Kerr Microscopy in polar mode, and Magnetic Force Microscopy (MFM) in Variable–Field (VF–MFM) mode, which allows us to probe structures down to sub–nm regime while applying

[a)]Authors to whom correspondence should be addressed: Elizabeth M Jefremovas: martinel@uni-mainz.de; Mathias Kläui: klaeui@uni-mainz.de

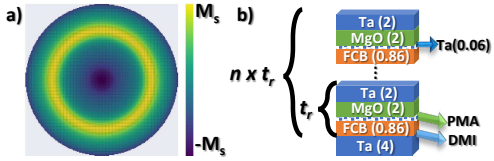

FIG. 1. **a)** Top-view of the magnetization of a 2π target skyrmion, also known as *skyrmionium*. Scale colour indicates the direction of the z component or the magnetization M, normalized to M_s. **b)** Scheme of the multilayer stack. Each multilayer unit, t_r, is composed by (from bottom to top) Ta, FCB ($Fe_{60}Co_{20}B_{20}$), MgO and Ta, number in brackets referring to the film thickness (in nm). Each unit is repeated n times to scale up the dipolar coupling. All samples are deposited on Si/SiO_2.

an OOP magnetic field. Details on the particular set up can be found in Ref.[22]. All the stacks were heated by a Peltier element equipped with a Pt100 sensor attached right next to the sample for temperature control between 280 and 380 K. The temperature stability was ensured to be within 0.1 K from 280 to 340 K, and within 1 K up to 380 K.

Fig. 2 provides an overview on the nucleation procedure of the TSk states in $n = 2$. To ease the tracking of the nucleated textures, while ensuring the reproducibility of the experiments, a 200 μm square has been patterned using Electron Beam Lithography. The large dimensions of the structure exclude significant lateral confinement effects (see Supplementary Material, Fig. S1). This strategy has enabled us to repeat systematically the described nucleation procedure excluding thermal drift or other error sources, confirming its validity and robustness against time.

The ground state of the system after saturation at RT = 292 K corresponds to a multidomain pattern, as it can be seen in the top left image, encircled in orange (Fig. 2). In order to activate TSk states using temperature fluctuations, the following nucleation procedure is followed: after in-plane (IP) saturation (IP field = 0.4 T), the sample temperature is stabilized at the values inserted at top row of Fig. 2 (307, 310 K...), and then, decreased back to RT. The top row of Fig. 2 shows that below $T = 314$ K, the sample relaxes back to a multidomain configuration without significant alteration of the domain periodicity. The situation changes drastically for $T \geq 314$ K (≈ 27 meV), when $k - \pi$ TSk states get activated, including $k = 1\pi$ (skyrmions), 2π (also known as *skyrmionium*) and even, 3π. Further increasing the thermal excitation to 320 or 327 K also yields TSks. In all cases, the number of TSks is on average the same, regardless the temperature value, indicating that the probability to nucleate TSk remains constant in the whole studied temperature range (≤ 327 K). This reveals that the energy landscape of our stack hosts metastable topological phases, protected by energy barriers that can be overcame at temperature ranges close to RT (see below Fig. 5). In addition to this, the TSks are nucleated at different positions in every re-nucleation for all the stacks [see Supplementary Material Fig. S1 **c)** and **d)**]. Therefore, there is no preference of some specific sites for the nucleation of the textures. This indicates a flat energy landscape of the sample, thus pinning is not the mechanism responsible for TSk nucleation, which constitutes a step forward compared to previous works[6,23,24]. Furthermore, our stack is also capable of stabilizing TSks following the reported strategy based on the geometrical confinement. As it can be seen in Fig. S1 in Supplementary Material, TSks are stabilized at zero field in 4 μm microdiscs, while the larger disks showcase a multidomain state with a similar domain periodicity of the continuous film (≈ 2 μm). This means that our stack can not only host TSk in confined geometries, yet it does in the continuous film, with boosts their implementation in technology applications.

We have tested the TSk stability against further thermal excitations. The middle panel of Fig. 2 provides an overview on the effects of temperature for the TSks. First, we have nucleated TSks by raising the temperature to 314 K. Then, we have decreased the temperature to RT and taken the first image (first in the row). After this, we have raised the temperature to 307 K, and decreased it to RT, where the measurement has been taken (second image in the row). Then, we have repeated the procedure for each temperature value up to 327 K. This is what we denote "temperature cycling". All measurements are performed at 0 field. As it can be seen in the whole series, the TSks are robust against temperature, as no significant changes are detected. We have also reversed the procedure, *i.e.*, starting the temperature cycling from highest T, and repeating the process until the lowest 307 K, obtaining the same results. An additional experiment has been performed, included in the Supplementary Material Fig. S2, confirming the reversibility of the temperature cycles.

We have further studied the stability of the TSks against out–of–plane (OOP) magnetic field. Our experimental results, included in the bottom panel of Fig. 2, illustrate the stability of the TSk up to 0.33 mT, where they collapse, but with a clear difference between the annihilation of even and odd k–π TSks. Fundamentally, there are only two types of k–π skyrmions, $k = 1$ ($\mathscr{W} = 1$), and $k = 2$ ($\mathscr{W} = 0$). All other TSks are built up as a combination of the two. This means that a 3π TSk is actually a 1π TSk wrapped by a 2π TSk, with no net topological charge. This implies a different collapse path for the structures, being the domains annihilated at lower fields than the inner skyrmion, which holds topological charge. As the OOP field is increased, the external 2π TSk shrinks progressively until it gets annihilated at 0.33 mT. On the contrary, the central 1π TSk remains, since its collapse requires going through an energetically highly unfavorable magnetic state, implying a higher energy to be annihilated[23,25,26]. This additional protection explains why at 0.56 mT, odd–π TSk still survive, while the even–ones have already collapsed. It is worth mentioning here the recent work by Nakamura *et al.*[27], where they propose to adopt the perspective of *communication between skyrmions*. This way, the annihilation path can be viewed as the energy competition

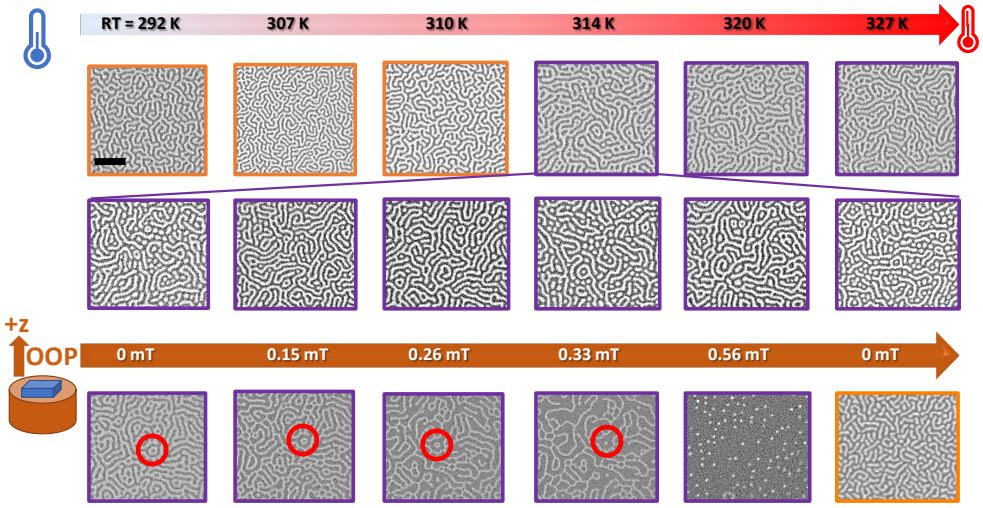

FIG. 2. Kerr Microscopy images of the TSks stabilized in a 200 μm square patterned for the $n = 2$ stack. Scale bar 10 μm is common for all images, dark (bright) contrast represents magnetization in $+z$ ($-z$) direction. All measurements are performed at RT = 292 K. Top (middle) panel evaluates the thermal nucleation (stability) of TSks at $\mu_0 H = 0$ mT OOP. Bottom panel evaluates the stability of the TSks under out of plane (OOP) magnetic field applied in $+z$ direction. Multidomain patterns (TSk) are enclosed in orange (purple). In bottom image, the annihilation of a TSk can be followed by the red circle.

between the opposite polarities (skyrmion core *vs.* ring). Higher rotations of the magnetization (k) would result into increased competition of polarities, ensuring a more robust TSk. After saturating the sample OOP, the system is restarted and a multidomain structure with no topological structures is formed at zero field, as shown in the bottom right figure.

Finally, we have tested the validity and robustness of our thermal-excitation TSk nucleation method against magneto-dipolar interactions. This constitutes an essential step to assess the validity of our proposed experimental methodology in building up a 3D spin texture, following the procedure stated by N. Kent *et al.*[23], where a 3D hopfion texture can be promoted by inserting a TSk in between two multilayer stacks with strong PMA, forcing the magnetization to wrap into the whole space. Important to note, the current experimental efforts for stabilizing 3D solitons notably rely on the expansion of the magnetic multilayer stack into the z-direction, as the multilayer stack allows to tune exchange, DMI, anisotropy or dipolar interactions. However, as a consequence of the increasing number of repetitions, the importance of the dipolar magnetostatic coupling raises, which could imply enhanced energy barriers protecting the TSk energy states. This would shift the thermal energy up, with the inherent thermal fluctuations, that could potentially prevent the stabilization of any spin texture that may be formed. In order to address this critical issue, we have reproduced the thermal-excitation nucleation procedure in 4 stacks with increasing number of repetitions, from $n = 3$ to $n = 12$, keeping the same composition as the one described before for $n = 2$ [Ta/CoFeB/MgO/Ta].

Fig. 3 includes representative images of TSk generated thermally in $n = 3$, 4, 7 and 12 repetitions. After saturation at room temperature, all the continuous films showed a multidomain maze-like pattern state. To nucleate the TSk, an OOP field was needed, unlike the case of $n = 2$, along with a higher temperature ramp. In such a way, we managed to nucleate TSk by an OOP field of $\mu_0 H = 0.73\pm0.01$, 6.30 ± 0.01, 11.8 ± 0.1, and 26.1 ± 0.1 mT in $n = 3$, 4, 7 and 12, at temperature values of 320, 327, 350 and 380 K, respectively. The systematic increase of the nucleation temperature with increasing number of repetitions (*i.e.*, dipolar interactions) indicates a higher energy barrier for the annihilation of the topological states, which agrees with magneto–dipolar coupling stabilizing role of spin textures[2,15,28,29]. Our experimental evidence points to the energy barrier to scale linearly with the number of repetition n as $E \propto 6.6 k_B n$, on first approximation. Assuming that the only sample parameter that changes from one stack to the other is the dipolar coupling[28], the linear dependence with n comes simply as a consequence of the increase of magnetic material, as already stated in the literature, *e.g.* Woo *et al.*[30]. It is worth mentioning that all the experiments are performed at temperature values far below the annealing point promoting structural changes ($\approx$ 520 K or even, higher[31]), and in no case did the magnetic properties

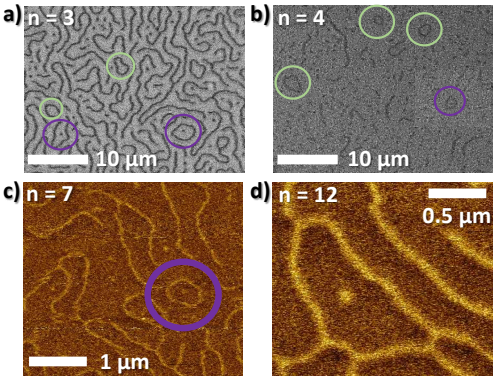

FIG. 3. Room temperature measurements of $n =$ **a)** 3, **b)** 4, **c)** 7 and **d)** 12 repetitions, nucleated at OOP field of $\mu_0 H = 0.73$, 6.3, 11.8, and 26.1 mT, respectively. Green circles enclose some of the 2π TSk, while the purple ones, the 3π TSk.

of the stack irreversibly change, as the multidomain state was always settled after saturation (see Supplementary Material Fig. S3).

We would like to highlight the existence of both 2π (see green circles in Fig. 3) and 3π–TSk states (purple circles), with a decrease in the occurrence as the number of k rotations increases. On average, the amount of 3π TSks is half the one of 2π-ones in $n = 3$, dropping to a fourth in $n = 4$. The dependence of the number of TSks with the number of repetitions n remains an interesting point that however needs to be reserved to a future study.

We have performed micromagnetic MuMax3 simulations[32] to understand the role thermal fluctuations in the nucleation of TSks. For these, we have used a 2 μm $\times$ 2 μm $\times$ 24 nm slice of material with similar magnetic properties as the CoFeB multilayer stacks at $n = 4$ (M_s = 600 kA/m, $K_u = 340$ kJ/m^3, $D = 0.9$ mJ/m^2 and $A = 10$ pJ/m, see[28]). The system was initialized to match experimental conditions (IP saturation, followed by an OOP field of 6 mT), and allowed to relax under the external field. We slightly varied the anisotropy between simulations to account for non-uniformity in material parameters, and focused on the time scale between nucleation and stabilization, which is in the order of tens of nanoseconds. None of our simulations has included an energy contribution associated to non-flat energy landscapes, excluding thus pining from the TSk nucleation. Six sets of simulations were performed for all material parameters: at T = 0, 100, 200, 300, 350 and 450 K. Our simulation results reveal the critical role of thermal fluctuations when the system relaxes from saturation, as no TSk is created at T = 0 K. In contrast, the system relaxes to a multidomain pattern regardless the anisotropy value, as shown in Fig. 4**a**, ensuring that the energy minima of the system is not the skyrmion lattice, *i.e.*, topological states are metastable states in our system. On the other hand side, in the presence of thermal fluctuations at T = 300 K, up to two TSks are nucleated and stabilized, as shown Fig. 4**b**. The result of our simulations are in good agreement with our experimental results, where the nucleation for the $n = 4$ stack is achieved at 327 K. Note the quantitative difference between simulations and experiments (300 K are enough to nucleate TSks in simulations, whereas 327 K are needed in experiments), which can result from the inherent inaccuracies of the micromagnetic model when applied to finite temperatures as well as uncertainties of the magnetic parameters. For instance, the values for A and D are taken from the literature for a similar stack composition[28,33–35], yet the actual ones from the sample can be slightly different, hampering a full quantitative 1:1 agreement between experiments and simulations. Still, the mismatch between simulation and experimental results is below 10%, which we consider sufficient for elucidating the critical role of temperature fluctuations in the nucleation of TSks in continuous films. We have further investigated the subtleties of this thermally activated process by analyzing the results of temperature values beyond the experimental capabilities, *i.e.*, from 0 to 450 K, represented in Fig. 4**c**). The percentage of TSk nucleated after saturation is zero below 300 K, as the thermal fluctuations are insufficient. At T = 300 K, the chance to get a TSk raises to 30%, yet further increase of the temperature yields a cut of the probability to 20% ($T = 350$ K), dropping to zero at 450 K. This reveals the fine balance of thermal fluctuations during the relaxation of the system. On the one hand, they need to deliver enough energy to overcome the energy barrier protecting the metastable states, on the other hand, they must keep moderated enough to let the nucleated TSks stabilize. Worth to mention, once nucleated, the TSks are stable and robust against temperature reduction and time, assuming no critical temperature dependence of the magnetic properties. Micromagnetic simulations show the prevalence of the TSks down to 0 K, revealing that temperature fluctuations play a role when the structure relaxes after saturation. Our experimental observations show that the TSks nucleated in $n =$ 7 remained unaltered for 4 months at RT and 0 field (see Fig. S4 in Supplementary Material).

To elucidate the role of thermal fluctuations in the nucleation process of the TSk metastable states, we have performed micromagnetic simulations focusing at very short time steps after nucleation from saturation. Fig. 5 includes the first 7 frames in time steps of 0.5 ns. We have identified that the starting point of the TSk nucleation is intimately related to the nucleation of skyrmions. As it can be seen, right immediately after saturation and heated up to 300 K, a skyrmion is nucleated (see t = 0.5 ns, encircled in red), as a consequence of the reduction of the PMA with the increase of the sample temperature, which renders topological metastable states accessible. Importantly, the process does not stop after the skyrmions are activated, but thermal fluctuations further deform the magnetic domains. As a result, a magnetic domain can encircle a skyrmion, (follow red circle in Fig. 5), which further stabilizes into a TSk provided the thermal fluctuations

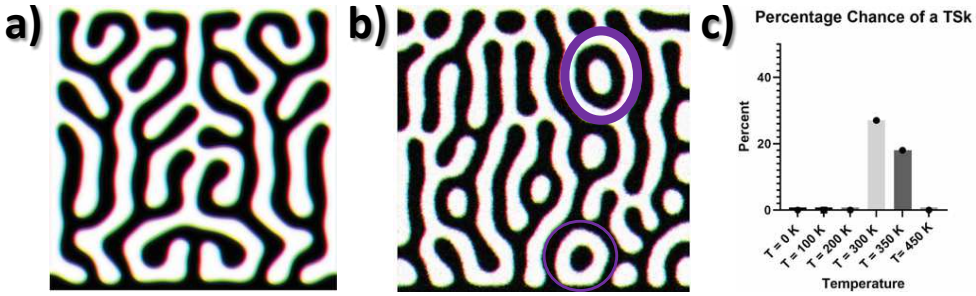

FIG. 4. MuMax3 Thermal Micromagnetic of the relaxed state of the system with an anisotropy of 340 kJ/m^3. Black and white represent spins in $+z$ and $-z$ direction, respectively **a)** T = 0 K, no TSks nor skyrmions observed in any simulation. **b)** T = 300 K. Two target skyrmions (encircled in purple) are stabilized. **c)** Percentage of TSks nucleated at T = 0, 100, 200 (none), 300 K (maximum), 350 K and 450 K (none). 11 simulations performed at each temperature.

are sufficient to overcome the domain wall repulsion and not too high to settle down a closed TSk, as it can be seen after 3.0 ns. A sketch of the process, starting from multidomain, ending up in TSk via skyrmion metastable state is captured in the bottom right sketch of this Fig. 5. Further increase of temperature provides higher thermal fluctuations, easing the path to overcome domain wall repulsion, in such a way as 3π TSks, or further topological states, can be accessed. However, at much higher temperatures, thermal fluctuations will overwhelm the skyrmion like core of the TSk, causing it to collapse, leaving just a normal skyrmion.

Starting from a magnetic multilayer stack, we have managed to nucleate TSk textures assisted by temperature fluctuations, with different topological charges in continuous films. The required temperature values are compliant with the ones of operating technological devices, and the described method is also valid for multilayer stacks comprising several repetitions in z direction. The created 1, 2 and 3π TSks are robust against temperature variations, low magnetic fields, dipolar coupling and time (months). Micromagnetic simulations on a material with similar properties as our stack support our results, showing a negligible probability of TSk nucleated at $T = 0$K, in contrast to the 30% chance of getting them at 300 K.

The crucial difference between our experimental system and previous ones, is that our nucleation method relies on no pinning or lateral confinement stabilizing TSk states, where all previous works did[6,10,23,24,36]. Our work proposes a completely different strategy, which does not depend on the particular pinning energy landscape of the sample and does not require from additional geometrical confinement, enabling the nucleated structures to move freely over the whole continuous film. This constitutes an enormous advantage for the envisioned spintronic devices, as the information carriers can freely move in all plane directions. On top of that, our multilayer stacks have been tuned to have nucleation temperatures between $\approx$ 300-350 K, *i.e.*, within the range

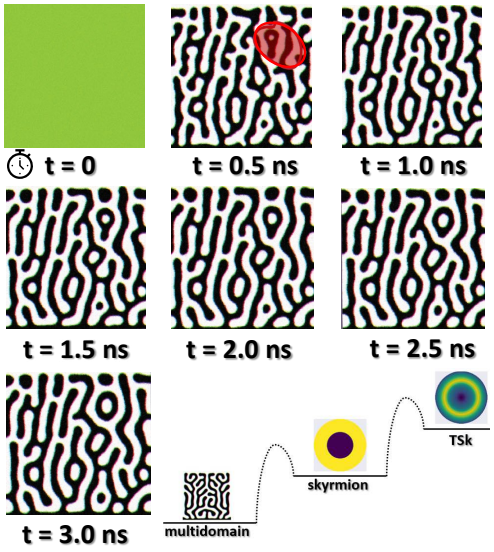

FIG. 5. Time-lapse of the nucleation of a target skymion according to nanomagnetic simulations, 0.5 ns snapshots. Encircled, the formation of a skyrmion, surrounded by a domain. After 3.0 ns, the structure is closed and forms a TSk. Bottom right a schematic showing relative energies of stable and metastable states in this system.

of operating values of technological devices. Our method also allows to reduce the topological charge of the structures via OOP magnetic fields, as TSk (2π) can be effectively converted to skyrmions (1π) within the mT range. This constitutes an additional advantage of our method towards applications, as the topological charge has a direct influence on carrier velocities and/on read/write information process.

Our engineered platform hosts TSk in continuous films of different orders, namely, 1, 2 and 3π. It remains an open question whether, at sufficiently high temperatures, higher order of TSk (5, 6, 7π etc.) would become enabled, as already hypothesized by Gao *et al.*[37]. Furthermore, our work enables the route for the experimental realization of hopfions *in continuous films*, as the closure of the magnetization rotation in the z dimension shall be forced by *encapsulating* the multilayer in between to two stacks with higher PMA, mimicking the strategy proposed for TSk confined in nanodisks by N. Kent *et al.*[15].

SUPPLEMENTARY MATERIAL

Supplementary Material includes extended information on the design of the multilayer stack; a comparison between the behaviour of continuous films *vs.* confined geometries; additional notes on the TSk stability against temperature, showcasing the case of reverse temperature cyclings; images corresponding to multidomain states at room temperature for the multilayers; and a representative MFM image of a TSk nucleated in $n = 7$ and stable after four months.

ACKNOWLEDGMENTS

EMJ acknowledges the "Alexander von Humboldt Postdoctoral Fellowship". Support from DFG (Priority Programme "Skyrmionics"), the ERC Synergy Grant 3D MAGiC (No. 856538) and the German Research Foundation (SFB TRR 173 Spin+X No 268565370, projects A01, B02 and A12) are acknowledged.

COMPETING INTERESTS

The authors declare no competing interests.

DATA AVAILABILITY

The data that support the findings of this study are available from the corresponding author upon reasonable request.

[1] J. P. Liu, Z. Zhang, and G. Zhao, *Skyrmions: Topological structures, properties, and applications* (CRC Press, 2016).
[2] A. Fert, N. Reyren, and V. Cros, "Magnetic skyrmions: advances in physics and potential applications," Nature Reviews Materials **2**, 1–15 (2017).
[3] G. Finocchio, F. Büttner, R. Tomasello, M. Carpentieri, and M. Kläui, "Magnetic skyrmions: from fundamental to applications," Journal of Physics D: Applied Physics **49**, 423001 (2016).
[4] K. Everschor-Sitte, J. Masell, R. M. Reeve, and M. Kläui, "Perspective: Magnetic skyrmions—Overview of recent progress in an active research field," Journal of Applied Physics **124** (2018).
[5] Z. Wang, Y. Su, S.-Z. Lin, and C. D. Batista, "Meron, skyrmion, and vortex crystals in centrosymmetric tetragonal magnets," Physical Review B **103**, 104408 (2021).
[6] F. Zheng, H. Li, S. Wang, D. Song, C. Jin, W. Wei, A. Kovács, J. Zang, M. Tian, Y. Zhang, *et al.*, "Direct imaging of a zero-field target skyrmion and its polarity switch in a chiral magnetic nanodisk," Physical Review Letters **119**, 197205 (2017).
[7] D. Cortés-Ortuño, N. Romming, M. Beg, K. Von Bergmann, A. Kubetzka, O. Hovorka, H. Fangohr, and R. Wiesendanger, "Nanoscale magnetic skyrmions and target states in confined geometries," Physical Review B **99**, 214408 (2019).
[8] S. Komineas and N. Papanicolaou, "Skyrmion dynamics in chiral ferromagnets," Physical Review B **92**, 064412 (2015).
[9] S. Li, J. Xia, X. Zhang, M. Ezawa, W. Kang, X. Liu, Y. Zhou, and W. Zhao, "Dynamics of a magnetic skyrmionium driven by spin waves," Applied Physics Letters **112** (2018).
[10] X. Zhang, J. Xia, Y. Zhou, D. Wang, X. Liu, W. Zhao, and M. Ezawa, "Control and manipulation of a magnetic skyrmionium in nanostructures," Physical Review B **94**, 094420 (2016).
[11] J. Tang, Y. Wu, W. Wang, L. Kong, B. Lv, W. Wei, J. Zang, M. Tian, and H. Du, "Magnetic skyrmion bundles and their current-driven dynamics," Nature Nanotechnology **16**, 1086–1091 (2021).
[12] B. Göbel, A. F. Schäffer, J. Berakdar, I. Mertig, and S. S. Parkin, "Electrical writing, deleting, reading, and moving of magnetic skyrmioniums in a racetrack device," Scientific reports **9**, 12119 (2019).
[13] K. Litzius, I. Lemesh, B. Krüger, P. Bassirian, L. Caretta, K. Richter, F. Büttner, K. Sato, O. A. Tretiakov, J. Förster, *et al.*, "Skyrmion hall effect revealed by direct time-resolved x-ray microscopy," Nature Physics **13**, 170–175 (2017).
[14] H. Vigo-Cotrina and A. Guimarães, "Switching of skyrmioniums induced by oscillating magnetic field pulses," Journal of Magnetism and Magnetic Materials **509**, 166895 (2020).
[15] N. Kent, N. Reynolds, D. Raftrey, I. T. Campbell, S. Virasawmy, S. Dhuey, R. V. Chopdekar, A. Hierro-Rodriguez, A. Sorrentino, E. Pereiro, *et al.*, "Creation and observation of hopfions in magnetic multilayer systems," Nature Communications **12**, 1562 (2021).
[16] M. Grelier, F. Godel, A. Vecchiola, S. Collin, K. Bouzehouane, A. Fert, V. Cros, and N. Reyren, "Three-dimensional skyrmionic cocoons in magnetic multilayers," Nature Communications **13**, 6843 (2022).
[17] K. Ran, Y. Liu, Y. Guang, D. M. Burn, G. van der Laan, T. Hesjedal, H. Du, G. Yu, and S. Zhang, "Creation of a chiral bobber lattice in helimagnet-multilayer heterostructures," Physical Review Letters **126**, 017204 (2021).
[18] P. Fischer, D. Sanz-Hernández, R. Streubel, and A. Fernández-Pacheco, "Launching a new dimension with 3d magnetic nanostructures," APL Materials **8** (2020).
[19] A. Fernández-Pacheco, R. Streubel, O. Fruchart, R. Hertel, P. Fischer, and R. P. Cowburn, "Three-dimensional nanomagnetism," Nature Communications **8**, 1–14 (2017).
[20] D. Marković, A. Mizrahi, D. Querlioz, and J. Grollier, "Physics for neuromorphic computing," Nature Reviews Physics **2**, 499–510 (2020).
[21] Z. Zhang, K. Lin, Y. Zhang, A. Bournel, K. Xia, M. Kläui, and W. Zhao, "Magnon scattering modulated by omnidirectional hopfion motion in antiferromagnets for meta-learning," Science advances **9**, eade7439 (2023).
[22] M. Jaafar, J. Gómez-Herrero, A. Gil, P. Ares, M. Vázquez, and A. Asenjo, "Variable-field magnetic force microscopy," Ultramicroscopy **109**, 693–699 (2009).
[23] N. Kent, R. Streubel, C.-H. Lambert, A. Ceballos, S.-G. Je, S. Dhuey, M.-Y. Im, F. Büttner, F. Hellman, S. Salahuddin, *et al.*, "Generation and stability of structurally imprinted target skyrmions in magnetic multilayers," Applied Physics Letters **115** (2019).
[24] Y. Zhang, M. Shi, W. Wang, X. Xu, M. Tian, D. Song, and H. Du, "Room-temperature zero-field kπ-skyrmions and their field-driven evolutions in chiral nanodisks," Nano Letters **23**, 10205–10212 (2023).
[25] S. Rohart, J. Miltat, and A. Thiaville, "Path to collapse for an isolated néel skyrmion," Physical Review B **93**, 214412 (2016).
[26] A. V. Ognev, A. G. Kolesnikov, Y. J. Kim, I. H. Cha, A. V. Sadovnikov, S. Nikitov, I. Soldatov, A. Talapatra, J. Mohanty, M. Mruczkiewicz, *et al.*, "Magnetic direct-write skyrmion nanolithography," ACS nano **14**, 14960–14970 (2020).
[27] K. Nakamura and A. O. Leonov, "Communicating skyrmions as the main mechanism underlying skyrmionium (meta) stability in quasi-two-dimensional chiral magnets," arXiv preprint arXiv:2404.10189 (2024).

[28]E. M. Jefremovas, K. Leutner, M. G. Fischer, J. Marqués-Marchán, T. B. Winkler, A. Asenjo, R. Frömter, J. Sinova, and M. Kläui, "The role of magnetic dipolar interactions in skyrmion lattices," arXiv preprint arXiv:2407.00539 (2024).
[29]J. Lucassen, M. J. Meijer, O. Kurnosikov, H. J. Swagten, B. Koopmans, R. Lavrijsen, F. Kloodt-Twesten, R. Frömter, and R. A. Duine, "Tuning magnetic chirality by dipolar interactions," Physical Review Letters **123**, 157201 (2019).
[30]S. Woo, K. Litzius, B. Krüger, M.-Y. Im, L. Caretta, K. Richter, M. Mann, A. Krone, R. M. Reeve, M. Weigand, *et al.*, "Observation of room-temperature magnetic skyrmions and their current-driven dynamics in ultrathin metallic ferromagnets," Nature materials **15**, 501–506 (2016).
[31]Y.-H. Wang, W.-C. Chen, S.-Y. Yang, K.-H. Shen, C. Park, M.-J. Kao, and M.-J. Tsai, "Interfacial and annealing effects on magnetic properties of cofeb thin films," Journal of Applied Physics **99** (2006).
[32]A. Vansteenkiste, J. Leliaert, M. Dvornik, M. Helsen, F. Garcia-Sanchez, and B. Van Waeyenberge, "The design and verification of mumax3," AIP Advances **4** (2014).
[33]J. Zázvorka, F. Jakobs, D. Heinze, N. Keil, S. Kromin, S. Jaiswal, K. Litzius, G. Jakob, P. Virnau, D. Pinna, *et al.*, "Thermal skyrmion diffusion used in a reshuffler device," Nature nanotechnology **14**, 658–661 (2019).
[34]A. Casiraghi, H. Corte-León, M. Vafaee, F. Garcia-Sanchez, G. Durin, M. Pasquale, G. Jakob, M. Kläui, and O. Kazakova, "Individual skyrmion manipulation by local magnetic field gradients," Communications Physics **2**, 145 (2019).
[35]Y. Ge, J. Rothörl, M. A. Brems, N. Kerber, R. Gruber, T. Dohi, M. Kläui, and P. Virnau, "Constructing coarse-grained skyrmion potentials from experimental data with iterative boltzmann inversion," Communications Physics **6**, 30 (2023).
[36]K. Ohara, X. Zhang, Y. Chen, Z. Wei, Y. Ma, J. Xia, Y. Zhou, and X. Liu, "Confinement and protection of skyrmions by patterns of modified magnetic properties," Nano Letters **21**, 4320–4326 (2021).
[37]Y. Gao, "Aging of magnetic skyrmions in a confined geometry," AIP Advances **14** (2024).